Approximations of the Helmholtz equation with variable wavenumber in one dimension

Dimitrios A. Mitsoudis[1,3], Michael Plexousakis[2,3], George N. Makrakis[2,3], and Charalambos Makridakis[2,3,4]

[1]Department of Naval Architecture, University of West Attica, Egaleo, Greece
[2]Department of Mathematics and Applied Mathematics, University of Crete, Heraklion, Greece
[3]Institute of Applied and Computational Mathematics, FORTH, Crete, Greece
[4]Mathematics Department, University of Sussex, Brighton, United Kingdom

August 1, 2024

Abstract

This work is devoted to the numerical solution of the Helmholtz equation with variable wavenumber and including a point source in appropriately truncated infinite domains. Motivated by a two-dimensional model, we formulate a simplified one dimensional model. We study its well posedness via wavenumber explicit stability estimates and prove convergence of the finite element approximations. As proof of concept, we present the outcome of some numerical experiments for various wavenumber configurations. Our experiments indicate that the introduction of the artificial boundary near the source and the associated boundary condition lead to an efficient model that accurately captures the wave propagation features.

Keywords: Helmholtz equation, variable wavenumber, finite elements, artificial boundary conditions

1 Introduction

The Helmholtz equation is a mathematical model for time-harmonic wave propagation and scattering problems and finds application in diverse fields like acoustics, electromagnetics, oceanography, and geophysics. Very often it is posed in infinite or very large (compared to the characteristic wavelength) domains as, for example, in problems in underwater acoustics where the marine environment is modeled as an infinite waveguide. The numerical solution of the Helmholtz equation in such domains remains a very interesting and challenging task and an active area of extensive research. In fact, the resolution of the Helmholtz equation in dimensions three for moderate to high wavenumbers and realistic geometries and/or boundary conditions is a problem where current computational methods are not yet capable to address efficiently.

In order to approximate the solution of the Helmholtz equation in an infinite domain with a direct numerical method, the domain first has to be truncated in some way and, in turn, an equivalent problem be posed in the resulting finite computational domain. A common approach for truncating an infinite domain is to introduce an artificial boundary that surrounds the region of interest for the wave phenomena that are studied, and derive appropriate absorbing boundary conditions (ABCs) to impose on this artificial boundary. In the ideal case, these ABCs aim to allow waves to leave the computational domain, as if they were propagating into an infinite one, without causing spurious reflections from the presence of the artificial boundary. Several types of ABCs exist, including local and nonlocal ABCs (see, e.g., the book by Givoli [12]) and perfectly matched layers (PML) [35, 21, 4]. Other numerical methods for these kinds of problems that have been developed and widely used during the last four decades include the use of absorbing layers, infinite elements, boundary integral methods, and various semi-analytical methods. Similar challenges arise in the important case where a point source emanating waves is included in the model. The treatment of artificial boundary conditions follows standard approaches, provided that the point source remains within the computational domain, but then the numerical treatment of the problem with finite elements becomes cumbersome due to the presence of a distribution as a source. Our aim is to systematically develop efficient finite element methods which simultaneously fulfill the following objectives: (i) they are able to handle realistic scenarios, including geometries and boundary conditions, (ii) point sources are included in the model, but lie outside the computational domain, and thus the derived model includes their effect on the boundary rather than as a distribution appearing in the right hand side of the principal part of the equation, and (iii) the resulting models are mathematically stable with wavenumber explicit constants [27, 29, 28]. Several challenges arise from both computational and analytical perspectives due to the mathematical structure of the problem. Notably, the model exhibits distinct behaviours in the near-field and far-field, even in one dimension, placing it in the class of scattering problems involving a *non-compact perturbation of the boundary.* The focus in this paper, is to consider the spatially dependent, variable wavenumber case, and as a proof of concept, to analyse the one-dimensional model problem, including finite element approximations.

Our model has interesting similarities, which will be further explored in a forthcoming work, with a problem of great importance appearing in several applications and concerning the understanding of the acoustic scattering effect of a non compact perturbation of the boundary of a flat two-dimensional waveguide, resulting to a non-uniform waveguide with different constant widths at infinity. In such a model, it is usually assumed that the acoustic field is generated by a harmonic point source located in a region with constant width. It is known that while scattering by bounded obstacles can be treated essentially by the same methods as the corresponding problem for the Schrödinger operator with short-range, even of compact support, potential, scattering by non compact obstacles acquires remarkable similarities with multi-particle quantum scattering, and different channels can be considered that correspond to different exits of the obstacle at infinity [36].

A two-dimensional waveguide problem.

To fix ideas, we describe first a two-dimensional problem. Then, in the forthcoming sections we shall study its simplified one-dimensional version. We consider the Green's function for the Helmholtz equation in a two-dimensional waveguide consisting of a single water layer overlying an acoustically-soft bottom of variable topography. The upper boundary of the waveguide is assumed to be a horizontal pressure-release surface. We introduce a Cartesian coordinate system (x, y), where the x-axis lies on the surface and the y-axis (depth) is taken to be positive downward, see Figure 1. The acoustic field is generated by a time-harmonic point source of frequency located at (x_s, y_s). We also assume that the inhomogeneities of the medium and the variable bottom topography are confined in range within an interval $[x_1, x_2]$. Specifically, we assume that the bottom is the graph of a sufficiently smooth, positive function h, such that $h(x) = D_N$, for $x \leq x_1$ and $h(x) = D_F$, for $x \leq x_2$, where $x_s < x_1 < x_2$ and D_N, D_F are positive constants.

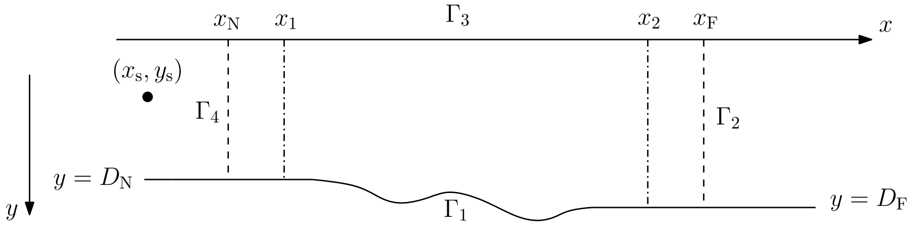

Figure 1: Schematic representation of the waveguide and basic notation.

In this model the acoustic field (usually acoustic pressure) satisfies the Helmholtz equation,[19]

$$-\Delta u(x, y) - k^2 u(x, y) = \delta(x - x_s)\delta(y - y_s), \tag{1.1}$$

where δ denotes the Dirac distribution and the (real) wavenumber k is a sufficiently smooth function of the form

$$k(x, y) = \begin{cases} k_N, & \text{for } x \leq x_1, \\ k_{\text{int}}(x, y), & \text{for } x_1 < x < x_2, \\ k_F, & \text{for } x \geq x_2. \end{cases}$$

Moreover, we assume that $k(x, y)$ is continuous and $0 < k_{min} < k(x, y) < k_{max}$ for all (x, y). Equation (1.1) is supplemented by homogeneous Dirichlet boundary conditions on the surface and on the bottom and by appropriate radiation conditions stating that

$$u(x, y) \text{ is ‘outgoing’ as } x \to \pm\infty.$$

When one is interested in solving this problem computationally with a direct numerical method, the original infinite domain has to be truncated. One way to achieve this is by introducing two artificial boundaries at some appropriate values of x, near the source (at $x = x_N \in (x_s, x_1)$) and far from the source (at $x = x_F > x_2$), denoted by Γ_4 and Γ_2, respectively. On these artificial boundaries suitable nonlocal conditions of DtN type may then be imposed, which are essentially derived from explicit solutions of the associated PDE problem in the semi-infinite strips ($x < x_1$ and $x > x_2$). Moreover, Ω, Γ_3 and Γ_1 denote the bounded part of the waveguide, of the surface and of the bottom, respectively, that are confined between $x = x_N$ and $x = x_F$. The construction of the DtN map at the boundaries $x = x_N, x_F$ is an involved procedure based on the analytical construction of the radiating wave fields in the half strips $x < x_N, x < x_F$. For example, at the boundary $x = x_F$, we get the condition

$$\frac{\partial u}{\partial x}(x_F, y) = T_1 u(y) + T_2 u(y),$$

where

$$T_1 u(y) := i \sum_{n=1}^{M_F} \sqrt{k_F^2 - \mu_n^F}\; u_n^F(x_F)\, Y_n^F(y) \;\text{ and }\; T_2 u(y) := - \sum_{n=M_F+1}^{\infty} \sqrt{\mu_n^F - k_F^2}\; u_n^F(x_F)\, Y_n^F(y).$$

Here, M_F is the finite number of propagating modes (waves oscillating at $x = +\infty$, as it is dictated by the radiation condition), and

$$\mu_n^F = \left(\frac{n\pi}{D_F}\right)^2, \quad Y_n^F = \sqrt{\frac{2}{D_F}} \sin \frac{n\pi y}{D_F}, \;\; n = 1, 2, \ldots, \quad u_m^F(x_F) := \int_0^{D_F} u(x_F, y)\, Y_m^F(y)\, dy,$$

are the eigenvalues, resp. the orthonormal eigenfunctions (that form a complete orthonormal system in $L^2(0, D_F)$ with respect to the standard inner product), and the corresponding Fourier coefficients of the wave field $u(x > x_F, y)$, respectively. The DtN condition at the boundary $x = x_N$ has a similar form, apart that it contains an extra term arising from the point source in $x < x_N$.

It is important to emphasize here that the waveguide problem described above is quite different from, and much more difficult, than the case of a locally perturbed waveguide, where $D_F = D_N$ and $k =$ const. for $x > x_F$ and $x < x_N$, and any perturbation either of the boundary (bottom) or/and of the wavenumber is confined in the region $x_N < x < x_F$. In the latter case the radiation conditions at $x = \pm\infty$ are the same, while in the former case, where $D_F \neq D_N$ or/and $k_F \neq k_N$, they are different on the left and the right. Therefore, when the perturbation of the waveguide is non local, we cannot exploit ideas and techniques from the theory of smooth compact perturbations [31] and "black box" scattering [9]. In order to understand the problem, it seems appropriate to look separately at the scattering mechanisms arising from the perturbation of the boundary and from the perturbation of the wavenumber. In this respect, we study in this paper the FEM solution of the simplified one dimensional problem of smooth non local perturbation of the homogeneous medium.

Literature review.

Finite element methods coupled with ABCs in unbounded waveguides can be traced back to the work of Fix and Marin [10], where they study the Helmholtz equation in a cylindrical semi-infinite waveguide and propose a finite element method coupled with a "generalized radiation condition" imposed on an artificial boundary. They used separation of variables to derive their outflow boundary condition which is now known as the Dirichlet-to-Neumann (DtN) boundary condition [20, 12]. Goldstein [13] introduced a finite element method for solving the Helmholtz equation in a perturbed semi-infinite cylindrical waveguide with a nonlocal ABC of the form $\partial u/\partial n = T(u)$, where n denotes the outward unit normal on the artificial boundary and T is the DtN map in the form of an eigenfunction series, He rigorously demonstrated the accuracy of the method and, moreover, he examined the effect on error estimates of truncating the infinite series appearing in the definition of T. Bayliss et al [3] considered the Helmholtz equation in a two-dimensional Cartesian waveguide with a suitable radiation condition at infinity. Their numerical experiments indicated that for a second-order method the error in the L^2 norm grows with the wavenumber k, when kh is kept constant, whereas it remains bounded for $k^3h^2 =$ const., where h is the mesh size. Bendali and Guillaume [5] introduced quasi-local non-reflecting boundary conditions for the Helmholtz equation in a semi-infinite waveguide that were perfectly transparent for all propagating modes. Athanassoulis et al. [1] considered an underwater sound propagation problem in a two-layered marine waveguide with (locally) range-dependent interface and locally variable sound speed, and compared the results of a coupled mode method with those of a finite element method in range-dependent test problems.

Frequency explicit stability and finite element error bounds are important, since may highlight subtle correlations between the wave number and the mesh size. Such detailed analysis was initiated by I. Babuška and his collaborators on mid 90's, for detailed experimental and theoretical studies of these works we refer to the book of Ihlenburg [17] and the references therein. The stability analysis based on energy methods via nonstandard test functions was considered in the works of Makridakis, Ihlenburg and Babuška [24] and Melenk [25]. Similar test functions were considered previously [30], and were instrumental in the derivation of a Rellich-type identity [8]. Such tools were employed in the case of a constant wavenumber, two-dimensional model problem [28]. The well-posedness was established under the assumption that the bottom is downsloping, i.e., it is described as an increasing function of the range x. A key step to this analysis was the derivation of a stability estimate that implied uniqueness which, in turn, inferred existence [24, 25, 15].

We are interested in analysing the model mentioned above in the case of a variable wavenumber that reflects time-harmonic wave propagation in an inhomogeneous medium. Variable wavenumber introduces a number of technical issues which we address in the one dimensional problem below. For related early works we refer to the work of Aziz et al. [2], where they proved a rigorous convergence theorem for a one-dimensional heterogeneous Helmholtz problem under the assumption that k^2h is sufficiently small. Makridakis et al. [24] considered a problem with piecewise constant material properties in one dimension. Recent works include the paper by Chaumont-Frelet [7] on high order methods for a one-dimensional problem with piecewise constant coefficients that allow for an arbitrary number of jumps, the work of Sauter and Torres [33] on the stability of a one-dimensional heterogenous Helmholtz equation for high frequencies with non-smooth and rapidly oscillating coefficients on a bounded interval, and the paper by Graham and Sauter [15], where they present the stability theory and the numerical analysis of the Helmholtz equation with variable coefficients of low regularity, in one to three space dimensions.

The rest of the paper is organized as follows. In Section 2 we describe the problem governed by the Helmholtz equation in the whole real line, with a harmonic point source located at some point $x = x_s$, and a wavenumber that may vary within a bounded interval that does not contain the source, while it assumes constant but different values elsewhere. Then we introduce two artificial boundaries near and far from the source, and we formulate an equivalent problem on the resulting bounded domain by imposing DtN-type conditions on the artificial boundaries. The derivation of the near-field boundary condition is discussed in detail. In Section 3 we describe the weak formulation of the problem, we introduce notation and prove some preliminary results. Section 4 is devoted to the well-posedness of the variational problem, that is established under an assumption that allows k to increase arbitrarily with x but imposes significant restriction on the oscillations that are allowed. However, this assumption and the use of a "Rellich"-type test function let us derive a stability estimate that implies uniqueness. Then existence is inferred by the Fredholm alternative. Let us remark here that well-posedness may be also obtained using the unique continuation principle, as in Graham and Sauter [15], without resorting to proving a stability estimate, but this approach does not lead to wavenumber explicit estimates. In the remaining part of this section we prove an inf-sup condition. Our approach allows for the reduction of the computational domain size (see Section 6), enabling the use of efficient computational methods for higher wavenumbers. In Section 5, we demonstrate that classical error analysis can be derived for finite element approximations of our model problem, with a focus on bounds that explicitly depend on the wavenumber. In Section 5.1, we derive error estimates for linear elements by calculating the dependence on the variable k of the corresponding mesh restrictions. In Section 5.2, we provide a more general stability and quasi-optimality analysis applicable to abstract discrete spaces. We employ standard arguments based on ideas introduced by Aziz et al. [2], Makridakis et al. [24], and Melenk [25], adapting the approach from Schatz [34]. The concept of the approximability of the dual problem, introduced by Sauter [32], is essential in Section 5.2. In Section 6, as a proof of concept, we present the outcome of some numerical experiments for various wavenumber configurations. Our experiments indicate that the introduction of the artificial boundary near the source and the associated boundary condition lead to an efficient model that accurately captures the wave propagation features.

2 Formulation

We consider the (locally) heterogeneous Helmholtz equation

$$-u'' - k^2(x)u = \delta(x - x_s), \quad x \in \mathbb{R}, \tag{2.1}$$

where δ is the Dirac distribution. We assume that the wavenumber k is a C^1 function that may vary in a bounded interval $[x_1, x_2]$, which does not include x_s, while it remains constant elsewhere, see the schematic representation in Figure 2. In particular, let $x_s < x_1 < x_2$ and

$$k(x) = \begin{cases} k_L & \text{for } x < x_1, \\ k_i(x) & \text{for } x_1 \le x \le x_2, \\ k_R & \text{for } x > x_2. \end{cases}$$

Moreover, we assume that $k(x)$ is bounded below and above by two strictly positive numbers $k_{\min}$ and

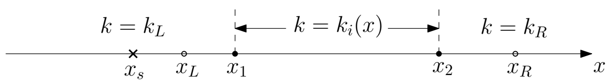

Figure 2: Schematic representation of the problem setup and basic notation. The cross indicates the location of the point source.

$k_{\max}$, respectively, i.e. $0 < k_{\min} \le k(x) \le k_{\max}$. Equation (2.1) is supplemented by the Sommerfeld radiation condition at $\pm\infty$, ensuring that the wave field is outgoing as $x \to \pm\infty$.

A common procedure for the numerical solution of problems of this type, with a direct numerical method, is to truncate the originally infinite domain by introducing an artificial boundary and applying suitable non-reflecting conditions on it. In this one-dimensional model problem a standard practice is to introduce two artificial boundaries at $x = x_L$ and $x = x_R$, so that the computational domain (x_L, x_R) includes the point source and the interval (x_1, x_2) where all the medium heterogeneities reside. Next, the classical Dirichlet-to-Neuman (DtN) boundary conditions may be imposed to the artificial boundaries ($x = x_L$ and $x = x_R$). In this simple one-dimensional case, outgoing waves at $\pm\infty$ satisfy the corresponding Sommerfeld condition at any finite x [12, 17], therefore the usual DtN boundary conditions are simply $u'(x_L) + ik_L u(x_L) = 0$ and $u'(x_R) - ik_R u(x_R) = 0$.

However, in the current setup we may further truncate the domain and introduce the artificial boundary at $x = x_L$ so that $x_s < x_L < x_1$. In this way, the source is outside the computational domain and an alternative condition must be imposed on the artificial boundary $x = x_L$, 'near' the source, that will account for the effect of the source and will also be 'transparent' (in the sense that it does not introduce spurious reflections) for left-going waves. In what follows, we present the derivation of this 'near-field' boundary condition.

2.1 Derivation of the 'near-field' boundary condition

Let $x < x_1$ and consider the associated homogeneous problem

$$-u'' - k_L^2 u = 0. \tag{2.2}$$

Equation (2.2) has two independent solutions $\varphi_1(x) = e^{ik_L x}$ and $\varphi_2(x) = e^{-ik_L x}$. The Wronskian is equal to $W(\varphi_1, \varphi_2) = -2ik_L$. Therefore, the solution of (2.1) for $x < x_1$ may be written as

$$\begin{aligned} u(x) &= a\, e^{ik_L x} + b\, e^{-ik_L x} + \int_{x_1}^{x} \frac{\varphi_1(\xi)\varphi_2(x) - \varphi_2(x)\varphi_1(\xi)}{-2ik_L}\, \delta(\xi - x_s)\, d\xi \\ &= a\, e^{ik_L x} + b\, e^{-ik_L x} - \frac{1}{2ik_L} \int_{x_1}^{x} \left(e^{ik_L \xi} e^{-ik_L x} - e^{ik_L x} e^{-ik_L \xi} \right) \delta(\xi - x_s)\, d\xi \\ &= a\, e^{ik_L x} + b\, e^{-ik_L x} - \frac{1}{2ik_L} \int_{x_1}^{x} \left(e^{-ik_L (x-\xi)} - e^{ik_L (x-\xi)} \right) \delta(\xi - x_s)\, d\xi. \end{aligned}$$

Case A: Let $x_s < x < x_1$. Then, $x_s \notin (x, x_1)$ and

$$u(x) = a\, e^{ik_L x} + b\, e^{-ik_L x}.$$

Case B: Let $x < x_s < x_1$. Then

$$
\begin{aligned}
u(x) &= a\, e^{ik_L x} + b\, e^{-ik_L x} - \frac{1}{2ik_L}\Big(e^{-ik_L(x-x_s)} - e^{ik_L(x-x_s)}\Big)\\
&= \big(a + \frac{1}{2ik_L}\, e^{-ik_L x_s}\big)\, e^{ik_L x} + \big(b - \frac{1}{2ik_L}\, e^{ik_L x_s}\big)\, e^{-ik_L x}.
\end{aligned}
$$

The term $e^{ik_L x}$ represents a right-going wave while the term $e^{-ik_L x}$ represents a left-going wave. Therefore, u is outgoing at $-\infty$ if

$$
a = -\frac{1}{2ik_L}\, e^{-ik_L x_s}.
$$

Hence, for $-\infty < x < x_s$ we have

$$
u(x) = \big(b - \frac{1}{2ik_L}\, e^{ik_L x_s}\big)\, e^{-ik_L x}.
$$

For $x_s < x < x_1$ we have

$$
u(x) = a\, e^{ik_L x} + b\, e^{-ik_L x} \quad \text{with} \quad a = -\frac{1}{2ik_L}\, e^{-ik_L x_s},
$$

so that

$$
u(x) = -\frac{1}{2ik_L}\, e^{ik_L(x-x_s)} + b\, e^{-ik_L x}. \tag{2.3}
$$

Differentiating (2.3), we get for $x_s < x < x_1$

$$
\begin{aligned}
u'(x) &= -\frac{1}{2ik_L}\, ik_l\, e^{ik_L(x-x_s)} - ik_L\, b\, e^{-ik_L x}\\
&\overset{(2.3)}{=} -\frac{1}{2}\, e^{ik_L(x-x_s)} - ik_L\Big(u(x) + \frac{1}{2ik_L}\, e^{ik_L(x-x_s)}\Big)\\
&= -ik_L u(x) - e^{ik_L(x-x_s)}.
\end{aligned}
$$

Now, the near-field non-homogeneous DtN-type boundary condition results by evaluating the above at $x = x_L$, for some $x_L \in (x_s, x_1)$

$$
u'(x_L) = -ik_L u(x_L) - e^{ik_L(x_L-x_s)}. \tag{2.4}
$$

Therefore, the original problem for (2.1) is replaced by the following equivalent problem posed in the bounded interval $\Omega := (x_L, x_R)$. We seek a complex-valued function u such that

$$
\begin{aligned}
-u'' - k^2(x)u &= 0, \quad x \in \Omega, && (2.5)\\
u'(x_L) &= -ik_L u(x_L) - e^{ik_L d}, && (2.6)\\
u'(x_R) &= ik_R u(x_R). && (2.7)
\end{aligned}
$$

where $d := x_L - x_s$ is the distance between the source and the near-field artificial boundary.

3 Weak formulation of the problem

Let $\mathcal{H} := H^1(\Omega)$ and denote by $\|\cdot\|$ the usual L^2-norm and by $\|\cdot\|_1$ the corresponding H^1-norm. We introduce the k-dependent norm

$$
\|u\|_{\mathcal{H}} = \Big(\|u'\|^2 + \|ku\|^2\Big)^{1/2} = \Big(\|u'\|^2 + \int_\Omega k^2(x)\, |u(x)|^2\, dx\Big)^{1/2}. \tag{3.1}
$$

Since $0 < k_{\min} \le k(x) \le k_{\max}$, $\|\cdot\|_{\mathcal{H}}$ is equivalent to the standard H^1-norm $\|\cdot\|_1$. Moreover, let $D := x_R - x_L$ denote the distance between the two artificial boundaries.

Let v be a test function in $H^1(\Omega)$. Multiply (2.5) by $\overline{v}$, integrate over (x_L, x_R), and use integration by parts and the boundary conditions (2.6), (2.7), to get

$$
\int_{x_L}^{x_R} \big(u'\overline{v}' - k^2(x)u\overline{v}\big)\, dx - ik_R u(x_R)\overline{v}(x_R) - ik_L u(x_L)\overline{v}(x_L) = e^{ik_L d}\, \overline{v}(x_L).
$$

We introduce the sesquilinear form

$$\mathcal{B}(u,v) := \int_{x_L}^{x_R} \left(u'\overline{v}' - k^2(x)u\overline{v}\right) dx - ik_R u(x_R)\overline{v}(x_R) - ik_L u(x_L)\overline{v}(x_L). \tag{3.2}$$

Let $u \in H^1(\Omega)$. Then the weak form of the problem (2.5)-(2.7) reads:

$$\mathcal{B}(u,v) = \mathcal{F}(v) \quad \text{for all } v \in H^1(\Omega), \tag{3.3}$$

where $\mathcal{F}$ is the antilinear functional defined by $\mathcal{F}(v) := e^{ik_L d}\,\overline{v}(x_L)$.

Lemma 3.1. *Let $v \in \mathcal{H}$.*

(i) It holds that

$$\|v\| \le \frac{1}{k_{\min}}\|v\|_{\mathcal{H}} \quad \textit{and} \quad \|v\|_1 \le C_1\|v\|_{\mathcal{H}}, \quad \textit{where } C_1 := \max\{1, \frac{1}{k_{\min}}\}. \tag{3.4}$$

(ii) The following trace inequality holds

$$|v(a)| \le \left(|v(x_L)|^2 + |v(x_R)|^2\right)^{1/2} \le C_2\,\|v\|^{1/2}\|v\|_1^{1/2} \le C_3\,\frac{1}{\sqrt{k_{\min}}}\,\|v\|_{\mathcal{H}}, \tag{3.5}$$

where $C_2 := 2^{3/4}\max\{1, \frac{1}{\sqrt{D}}\}$, $C_3 := C_1^{1/2}C_2$, and a is either of the endpoints x_L, x_R of Ω.

Proof. (i) Since $v \in \mathcal{H}$,

$$\|v\|^2 \le \frac{1}{k_{\min}^2}\|kv\|^2 \le \frac{1}{k_{\min}^2}\left(\|v'\|^2 + \|kv\|^2\right) = \frac{1}{k_{\min}^2}\|v\|_{\mathcal{H}}^2,$$

$$\|v\|_1^2 \le \|v'\|^2 + \frac{1}{k_{\min}^2}\|kv\|^2 \le \max\{1, \frac{1}{k_{\min}^2}\}\|v\|_{\mathcal{H}}^2.$$

(ii) Consider the integral $\int_\Omega \left(h\,|v|^2\right)_x$ where h is the linear function $h(x) := \frac{2}{D}(x - x_L) - 1$, so that $h(x_L) = -1$ and $h(x_R) = 1$, [15]. Using the fact that $\mathrm{Re}\{v\overline{v}'\} = \frac{1}{2}(|v|^2)_x$, the Cauchy-Schwarz inequality, the elementary inequality $\alpha + \beta \le \sqrt{2}(\alpha^2 + \beta^2)^{1/2}$, and (3.4), we get that

$$\begin{aligned}
|v(x_R)|^2 + |v(x_L)|^2 &= \int_{x_L}^{x_R}\left(h\,|v|^2\right)_x = \int_{x_L}^{x_R} h\,(|v|^2)_x + \frac{2}{D}\int_{x_L}^{x_R}|v|^2 = 2\int_{x_L}^{x_R} h\ \mathrm{Re}\{v\overline{v}'\} + \frac{2}{D}\,\|v\|^2 \\
&\le 2\int_{x_L}^{x_R}|h|\,|v|\,|v'| + \frac{2}{D}\,\|v\|^2 \le 2\|v\|\|v'\| + \frac{2}{D}\,\|v\|^2 = 2\|v\|\left(\|v'\| + \frac{1}{D}\,\|v\|\right) \\
&\le 2\max\{1, \frac{1}{D}\}\|v\|\left(\|v'\| + \|v\|\right) \le 2\sqrt{2}\max\{1, \frac{1}{D}\}\|v\|\|v\|_1 \\
&\le 2\sqrt{2}\max\{1, \frac{1}{D}\}\,C_1\,\frac{1}{k_{\min}}\,\|v\|_{\mathcal{H}}^2.
\end{aligned}$$

□

Proposition 3.1. *For all $u, v \in \mathcal{H}$, $\mathcal{B}$ is a bounded sesquilinear form with*

$$|\mathcal{B}(u,v)| \le C_4\|u\|_{\mathcal{H}}\|v\|_{\mathcal{H}}, \quad \textit{where } C_4 = 1 + C_3^2\,\frac{k_L + k_R}{k_{\min}}, \tag{3.6}$$

and satisfies a Gårding inequality

$$\mathrm{Re}\,\mathcal{B}(u,u) \ge \|u\|_{\mathcal{H}}^2 - 2k_{\max}^2\|u\|^2. \tag{3.7}$$

Proof.

$$\begin{aligned}
|\mathcal{B}(u,v)| &\le |\int_{x_L}^{x_R} u'\overline{v}'\,dx| + |\int_{x_L}^{x_R} k^2(x)u\overline{v}\,dx| + k_R|u(x_R)\overline{v}(x_R)| + k_L|u(x_L)\overline{v}(x_L)| \\
&\le \|u'\|\|v'\| + \|ku\|\|kv\| + k_R|u(x_R)||v(x_R)| + k_L|u(x_L)||v(x_L)|.
\end{aligned}$$

Hölder's inequality and (3.5) imply that

$$|\mathcal{B}(u,v)| \le \|u\|_{\mathcal{H}}\|v\|_{\mathcal{H}} + \frac{C_3^2}{k_{\min}}\, k_R\|u\|_{\mathcal{H}}\|v\|_{\mathcal{H}} + \frac{C_3^2}{k_{\min}}\, k_L\|u\|_{\mathcal{H}}\|v\|_{\mathcal{H}} = \big(1 + C_3^2\,\frac{k_L+k_R}{k_{\min}}\big)\,\|u\|_{\mathcal{H}}\|v\|_{\mathcal{H}}.$$

Moreover,

$$\operatorname{Re}\mathcal{B}(u,u) = \int_{x_L}^{x_R} (|u'|^2 - k^2(x)|u|^2)\,dx = \|u\|_{\mathcal{H}}^2 - 2\int_{x_L}^{x_R} k^2(x)|u|^2\,dx \ge \|u\|_{\mathcal{H}}^2 - 2k_{\max}^2\|u\|^2.$$

□

4 Well-posedness of the variational problem

Assumption. Suppose that there exists some $\theta > 0$ such that

$$1 + (x - x_L)\,\frac{k'(x)}{k(x)} \ge \theta > 0. \tag{4.1}$$

Theorem 4.1. *Assume that* (4.1) *holds and let* $u \in H^2(\Omega)\cap\mathcal{H}$ *be a solution of* (3.3)*. Then,*

$$\|u\|_{\mathcal{H}} \le C_5(k,\theta,D), \quad \textit{where} \;\; C_5 = \frac{C_3}{\theta\sqrt{k_{\min}}}\big(|1-\theta| + 2k_R D\big). \tag{4.2}$$

Proof. Consider the 'Rellich' test function $w(x) := (x - x_L)u'(x) + \alpha u(x)$, where α is a real constant. Clearly, $w'(x) = (x - x_L)u''(x) + (\alpha+1)u'(x)$. Then,

$$\begin{aligned}
\mathcal{B}(u,w) &= \int_{x_L}^{x_R} \big(u'\bar{w}' - k^2(x)u\bar{w}\big)\,dx - ik_R u(x_R)\overline{w}(x_R) - ik_L u(x_L)\,\underbrace{\overline{w}(x_L)}_{=\alpha\overline{u}(x_L)} \\
&= \int_{x_L}^{x_R} u'\big[(\alpha+1)\bar{u}' + (x-x_L)\bar{u}''\big]\,dx - \int_{x_L}^{x_R} k^2(x)\,u\,\big[(x-x_L)\,\bar{u}' + \alpha\bar{u}\big]\,dx \\
&\quad - ik_R u(x_R)\big[\underbrace{(x_R - x_L)}_{=D}\;\underbrace{\overline{u}'(x_R)}_{=-ik_R\overline{u}(x_R)}\; + \alpha\overline{u}(x_R)\big] - i\alpha k_L|u(x_L)|^2 \\
&= (\alpha+1)\int_{x_L}^{x_R} |u'|^2\,dx - \alpha\int_{x_L}^{x_R} k^2(x)\,|u|^2\,dx + \int_{x_L}^{x_R} (x-x_L)u'\bar{u}''\,dx \\
&\quad - \int_{x_L}^{x_R} (x-x_L)\,k^2(x)\,u\bar{u}'\,dx - k_R^2\,D\,|u(x_R)|^2 - i\alpha k_R|u(x_R)|^2 - i\alpha k_L|u(x_L)|^2.
\end{aligned}$$

Recall that $\operatorname{Re}\{u\bar{u}'\} = \frac{1}{2}\big(|u|^2\big)_x$ and $\operatorname{Re}\{u'\bar{u}''\} = \frac{1}{2}\big(|u'|^2\big)_x$. Therefore, taking real parts, we have that

$$\begin{aligned}
\operatorname{Re}\mathcal{B}(u,w) &= (\alpha+1)\int_{x_L}^{x_R} |u'|^2\,dx - \alpha\int_{x_L}^{x_R} k^2(x)\,|u|^2\,dx \\
&\quad + \int_{x_L}^{x_R} (x-x_L)\operatorname{Re}\{u'\bar{u}''\}\,dx - \int_{x_L}^{x_R} (x-x_L)\,k^2(x)\,\operatorname{Re}\{u\bar{u}'\}\,dx - k_R^2\,D\,|u(x_R)|^2 \\
&= (\alpha+1)\int_{x_L}^{x_R} |u'|^2\,dx - \alpha\int_{x_L}^{x_R} k^2(x)\,|u|^2\,dx \\
&\quad + \frac{1}{2}\int_{x_L}^{x_R} (x-x_L)\,\big(|u'|^2\big)_x\,dx - \frac{1}{2}\int_{x_L}^{x_R} (x-x_L)\,k^2(x)\,\big(|u|^2\big)_x\,dx - k_R^2\,D\,|u(x_R)|^2.
\end{aligned}$$

We integrate by parts to deduce that

$$\begin{aligned}
\frac{1}{2}\int_{x_L}^{x_R} (x-x_L)\,\big(|u'|^2\big)_x\,dx &= \left[\frac{1}{2}\,(x-x_L)\,|u'(x)|^2\right]_{x_L}^{x_R} - \frac{1}{2}\int_{x_L}^{x_R} |u'|^2\,dx \\
&= \frac{1}{2}\,D\,\underbrace{|u'(x_R)|^2}_{=k_R^2|u(x_R)|^2} - \frac{1}{2}\int_{x_L}^{x_R} |u'|^2\,dx \\
&= \frac{1}{2}\,D\,k_R^2|u(x_R)|^2 - \frac{1}{2}\int_{x_L}^{x_R} |u'|^2\,dx,
\end{aligned}$$

and

$$\frac{1}{2}\int_{x_L}^{x_R}(x-x_L)\,k^2(x)\,\big(|u|^2\big)_x\,dx = \left[\frac{1}{2}\,(x-x_L)\,k^2(x)\,|u(x)|^2\right]_{x_L}^{x_R} - \frac{1}{2}\int_{x_L}^{x_R}\big((x-x_L)k^2(x)\big)'\,|u|^2\,dx$$

$$= \frac{1}{2}\,D\,k_R^2\,|u(x_R)|^2 - \frac{1}{2}\int_{x_L}^{x_R} k^2(x)\,|u|^2\,dx$$

$$- \frac{1}{2}\int_{x_L}^{x_R}(x-x_L)\,2\,k(x)\,k'(x)\,|u|^2\,dx.$$

Hence,

$$\begin{aligned}\operatorname{Re}\mathcal{B}(u,w) = {} & (\alpha+1)\int_{x_L}^{x_R}|u'|^2\,dx - \alpha\int_{x_L}^{x_R}k^2(x)\,|u|^2\,dx + \frac{1}{2}\,D\,k_R^2|u(x_R)|^2 - \frac{1}{2}\int_{x_L}^{x_R}|u'|^2\,dx \\ & - \frac{1}{2}\,D\,k_R^2\,|u(x_R)|^2 + \frac{1}{2}\int_{x_L}^{x_R}k^2(x)\,|u|^2\,dx \\ & + \frac{1}{2}\int_{x_L}^{x_R}k^2(x)\,(x-x_L)\,2\,\frac{k'(x)}{k(x)}\,|u|^2\,dx - k_R^2\,D\,|u(x_R)|^2 \\ = {} & \big(\alpha+\frac{1}{2}\big)\int_{x_L}^{x_R}|u'|^2\,dx + \frac{1}{2}\int_{x_L}^{x_R}k^2(x)\left[1+2\,(x-x_L)\,\frac{k'(x)}{k(x)} - 2\alpha\right]|u|^2\,dx - k_R^2\,D\,|u(x_R)|^2.\end{aligned}$$

Now take $\alpha = -\frac{1}{2}+\frac{\theta}{2}$. (Of course, $\alpha+\frac{1}{2}=\frac{\theta}{2}$ and $1-2\alpha = 2-\theta$.) Then,

$$\operatorname{Re}\mathcal{B}(u,w) = \frac{\theta}{2}\,\|u'\|^2 + \frac{1}{2}\int_{x_L}^{x_R}k^2(x)\left(2+2\,(x-x_L)\,\frac{k'(x)}{k(x)}-\theta\right)|u|^2\,dx - k_R^2\,D\,|u(x_R)|^2. \tag{4.3}$$

Since (4.1) holds, it turns out that $2+2\,(x-x_L)\,\frac{k'(x)}{k(x)}-\theta \geq \theta$ for all $x\in[x_L,x_R]$. This implies the estimate

$$\frac{\theta}{2}\,\|u'\|^2 + \frac{\theta}{2}\int_{x_L}^{x_R}k^2(x)\,|u|^2\,dx \leq \operatorname{Re}\mathcal{B}(u,w) + k_R^2\,D\,|u(x_R)|^2 \;\Rightarrow\; \frac{\theta}{2}\,\|u\|_{\mathcal{H}}^2 \leq |\mathcal{B}(u,w)| + k_R^2\,D\,|u(x_R)|^2.$$

Recall that $|\mathcal{B}(u,w)| = |\mathcal{F}(w)| = |e^{ik_Ld}||w(x_L)| = |\alpha||u(x_L)| = |\frac{1-\theta}{2}||u(x_L)|$. Therefore

$$\frac{\theta}{2}\,\|u\|_{\mathcal{H}}^2 \leq \frac{|1-\theta|}{2}\,|u(x_L)| + k_R^2\,D\,|u(x_R)|^2. \tag{4.4}$$

It also holds that

$$-\operatorname{Im}\mathcal{B}(u,u) = k_R|u(x_R)|^2 + k_L|u(x_L)|^2. \tag{4.5}$$

Hence

$$k_R^2\,D\,|u(x_R)|^2 \leq k_R\,D\left(k_R|u(x_R)|^2 + k_L|u(x_L)|^2\right) = -k_R\,D\,\operatorname{Im}\mathcal{B}(u,u),$$

from which we have

$$k_R^2\,D\,|u(x_R)|^2 \leq k_R\,D\,|\mathcal{B}(u,u)| = k_RD\,|\mathcal{F}(u)| = k_RD\,|u(x_L)|. \tag{4.6}$$

Therefore, (4.4), (4.6), and (3.5), imply that

$$\frac{\theta}{2}\,\|u\|_{\mathcal{H}}^2 \leq \left(\frac{|1-\theta|}{2}+k_RD\right)|u(x_L)| \leq \left(\frac{|1-\theta|}{2}+k_RD\right)\frac{C_3}{\sqrt{k_{\min}}}\,\|u\|_{\mathcal{H}},$$

that is,

$$\|u\|_{\mathcal{H}} \leq \frac{C_3}{\theta\sqrt{k_{\min}}}\big(|1-\theta|+2k_RD\big).$$

□

Remark 4.1. The *virial* condition (4.1) can be formally derived from a well-known quantum non-trapping estimate applied to the homogeneous version of the Helmholtz equation (2.2). Let k_0 be any fixed reference wavenumber and $\eta(x) = k^2(x)/k_0^2$. We rewrite the homogeneous Helmholtz equation in the form of a Schrödinger equation $-u'' + V(x) = Eu(x)$, where $V(x) = k_0^2(1-\eta(x))$ and $E = k_0^2$. The quantum non-trapping condition (see equation (21.9) in Section 21.1 of Hislop and Sigal [16]) requires $S_E(x; V; \upsilon) := 2\upsilon'(x)(E - V(x)) - \upsilon(x)V'(x) \geq \epsilon_0$ for some $\epsilon_0 > 0$, and a smooth function $\upsilon(x)$. Thus, we get the condition

$$k_0^2(2\upsilon'\eta + \upsilon\eta') \geq \epsilon_0 \ . \tag{4.7}$$

Here, we make the special choice $\upsilon(x) = x - x_L$, which implies

$$2\eta + (x - x_L)\eta' \geq \epsilon_0/k_0^2. \tag{4.8}$$

By substituting $\eta = k^2(x)/k_0^2$ in the last inequality we derive (4.1) with $\theta = \epsilon_0/2k_{max}^2$.

The solution of the differential inequality (4.7) is $\upsilon(x) = \frac{1}{2k_0^2}\eta^{-1/2}(x)\int_{\alpha_0}^{x}\alpha(s)\eta^{-1/2}(s)ds$, $\alpha_0 \leq x < \infty$, where $\alpha(s) \geq \epsilon_0$ is an unspecified function which can be chosen according to a particular problem. Then, $S_E(x; V; \upsilon) = \alpha(x), \alpha_0 \leq x < \infty$. Note that Aziz et al. [2] use such function υ with $\alpha(s) \equiv 1$ in the proof of Lemma 2.1.

A multidimensional version of condition (4.8) is required for the proof of Theorem 2.19 in Graham et al. [14], where they study the 2D and 3D exterior problem for the Helmholtz equation in a heterogeneous medium by using Morawetz's multipliers. An instructive explanation of this condition, on the basis of geometrical optics, is given in Section 7 of this paper. To the best of our knowledge, this virial condition appeared for first time in the works of Kucherenko [22, 23] where he constructed the short-wave asymptotic expansion of Green's function for the multidimensional Helmholtz equation in inhomogeneous medium and the stationary Schrödinger equation.

Remark 4.2. The use of the standard test function $w(x) = (x - x_L)u'(x)$ would require the assumption $1 + 2(x - x_L)\frac{k'(x)}{k(x)} \geq \theta' > 0$. Note that in two and three dimensions [14], the use of the analogous test function $w(x) = x \cdot \nabla u$ requires again the assumption $1 + \frac{x\cdot\nabla k(x)}{k(x)} \geq \theta'' > 0$.

Remark 4.3. The case $\theta \geq 1$ in assumption (4.1) forces k to be strictly increasing. Therefore, to allow some oscillatory behavior for k, in practice we will assume that $0 < \theta < 1$.

Proposition 4.1. *Assume that* (4.1) *holds and let $u \in H^2(\Omega) \cap \mathcal{H}$ be a solution of $\mathcal{B}(u, v) = 0$, for all $v \in \mathcal{H}$. Then, $u = 0$ a.e. in Ω.*

Proof. Take $v = u$. Then (4.5) implies that $k_R|u(x_R)|^2 + k_L|u(x_L)|^2 = 0$, i.e. $u(x_R) = u(x_L) = 0$. In turn, (4.4) shows that $\|u\|_{\mathcal{H}}^2 \leq 0$. ☐

Proposition 4.1 implies uniqueness for the problem (3.3). Existence follows from Gårding inequality (3.7) and the Fredholm alternative.

In the remaining of this section we will prove a stability result for an auxiliary problem which will allow us to establish an inf-sup condition for the sesquilinear form (3.2).

Proposition 4.2. *Assume that* (4.1) *holds and let $u \in H^2(\Omega) \cap \mathcal{H}$ be a solution of*

$$\mathcal{B}(u, v) = (f, v) \quad \textit{for all } v \in \mathcal{H}, \tag{4.9}$$

for some $f \in L^2(\Omega)$. Then

$$\|u\|_{\mathcal{H}} \leq C_6(k, \theta, D)\|f\|, \quad \textit{where } C_6 = \frac{2\sqrt{2}D\max\left\{1, \frac{k_R}{k_{\min}}\left(1 + \frac{|1-\theta|}{2k_R D}\right)\right\}}{\theta}. \tag{4.10}$$

Furthermore, $u \in H^2(\Omega)$ and

$$\|u''\| \leq (1 + C_6 k_{\max})\|f\|. \tag{4.11}$$

Proof. As in the proof of Theorem 4.1, we consider the 'Rellich' test function $w(x) = (x - x_L)u'(x) + \frac{\theta-1}{2}u(x)$. Using the same arguments as before we may prove that

$$\frac{\theta}{2}\|u'\|^2 + \frac{\theta}{2}\int_{x_L}^{x_R} k^2(x)\,|u|^2\,dx \leq |\mathcal{B}(u, w)| + k_R D\,|\mathcal{B}(u, u)| = |(f, w)| + k_R D\,|(f, u)|.$$

Obviously, $|(f,u)| \le \frac{1}{k_{\min}}\|f\|\|ku\|$, and since $w(x) = (x-x_L)u'(x) + \frac{\theta-1}{2}u(x)$ we have that

$$\begin{aligned}
|(f,w)| &= \Big|\int_{x_L}^{x_R} \big[(x-x_L)f(x)\bar{u}'(x) + \frac{\theta-1}{2}\bar{u}(x)\big]\,dx\Big| \\
&\le D\Big|\int_{x_L}^{x_R} f(x)\bar{u}'(x)\,dx\Big| + \frac{|1-\theta|}{2}\Big|\int_{x_L}^{x_R} f(x)\bar{u}(x)\,dx\Big| \\
&\le D\,\|f\|\|u'\| + \frac{|1-\theta|}{2k_{\min}}\,\|f\|\|ku\|.
\end{aligned}$$

Using the relations above we get that

$$\begin{aligned}
\frac{\theta}{2}\,\|u\|_{\mathcal{H}}^2 &\le D\,\|f\|\|u'\| + \Big(\frac{|1-\theta|}{2k_{\min}} + \frac{k_R D}{k_{\min}}\Big)\,\|f\|\|ku\| \\
&= D\,\|f\|\|u'\| + \frac{k_R}{k_{\min}}\Big(1+\frac{|1-\theta|}{2k_R D}\Big)\,D\,\|f\|\|ku\| \\
&= 2\frac{\sqrt{\varepsilon}}{2}\Big[\|u'\| + \frac{k_R}{k_{\min}}\Big(1+\frac{|1-\theta|}{2k_R D}\Big)\|ku\|\Big]\,\frac{D}{\sqrt{\varepsilon}}\,\|f\| \\
&\le \frac{\varepsilon}{4}\Big[\|u'\| + \frac{k_R}{k_{\min}}\Big(1+\frac{|1-\theta|}{2k_R D}\Big)\|ku\|\Big]^2 + \frac{D^2}{\varepsilon}\,\|f\|^2 \\
&\le \frac{\varepsilon}{2}\Big[\|u'\|^2 + \Big(\frac{k_R}{k_{\min}}\Big)^2\Big(1+\frac{|1-\theta|}{2k_R D}\Big)^2\|ku\|^2\Big] + \frac{D^2}{\varepsilon}\,\|f\|^2 \\
&\le \frac{\varepsilon}{2}\,\max\Big\{1, \Big(\frac{k_R}{k_{\min}}\Big)^2\Big(1+\frac{|1-\theta|}{2k_R D}\Big)^2\Big\}\,\|u\|_{\mathcal{H}}^2 + \frac{D^2}{\varepsilon}\,\|f\|^2,
\end{aligned}$$

where ε is an appropriately small positive number. Therefore,

$$\Big(\theta - \varepsilon\,\max\Big\{1, \Big(\frac{k_R}{k_{\min}}\Big)^2\Big(1+\frac{|1-\theta|}{2k_R D}\Big)^2\Big\}\Big)\,\|u\|_{\mathcal{H}}^2 \le \frac{2D^2}{\varepsilon}\,\|f\|^2.$$

Now we choose ε such that $\varepsilon\,\max\Big\{1, \Big(\frac{k_R}{k_{\min}}\Big)^2\Big(1+\frac{|1-\theta|}{2k_R D}\Big)^2\Big\} = \frac{\theta}{2}$. Then,

$$\begin{aligned}
\frac{\theta}{2}\,\|u\|_{\mathcal{H}}^2 \le \frac{2D^2}{\varepsilon}\,\|f\|^2 &= \frac{4D^2\max\big\{1, \big(\frac{k_R}{k_{\min}}\big)^2\big(1+\frac{|1-\theta|}{2k_R D}\big)^2\big\}}{\theta}\,\|f\|^2 \\
\Rightarrow \|u\|_{\mathcal{H}}^2 &\le \frac{8D^2\max\big\{1, \big(\frac{k_R}{k_{\min}}\big)^2\big(1+\frac{|1-\theta|}{2k_R D}\big)^2\big\}}{\theta^2}\,\|f\|^2 \\
\Rightarrow \|u\|_{\mathcal{H}} &\le \frac{2\sqrt{2}D\max\big\{1, \frac{k_R}{k_{\min}}\big(1+\frac{|1-\theta|}{2k_R D}\big)\big\}}{\theta}\,\|f\|.
\end{aligned}$$

To prove (4.11), note that u is also a (strong) solution to the problem:

$$\begin{aligned}
&-u'' - k^2(x)u = f, \quad x \in \Omega, \\
&u'(x_L) = -ik_L u(x_L), \\
&u'(x_R) = ik_R u(x_R).
\end{aligned}$$

Hence, $u \in H^2(\Omega)$ and

$$\begin{aligned}
\|u''\| &\le \|k^2 u\| + \|f\| \le k_{\max}\|ku\| + \|f\| \le k_{\max}\|u\|_{\mathcal{H}} + \|f\| \\
&\overset{(4.10)}{\le} C_6 k_{\max}\|f\| + \|f\| = (1 + C_6 k_{\max})\|f\|.
\end{aligned}$$

□

Theorem 4.2 (Inf-sup condition)**.** *Assume that* (4.1) *holds. Then, the sesquilinear form* $\mathcal{B}(\cdot,\cdot)$ *defined on* $\mathcal{H}\times\mathcal{H}$ *satisfies*

$$\sup_{0\neq v\in\mathcal{H}} \frac{\operatorname{Re}\mathcal{B}(u,v)}{\|v\|_{\mathcal{H}}} \ge \frac{1}{k_{\min}}\Big(\frac{1}{k_{\min}} + C_7\Big)^{-1}\|u\|_{\mathcal{H}} \quad \text{for all } \ u \in \mathcal{H}, \tag{4.12}$$

where

$$C_7 := \frac{4\sqrt{2}D\max\big\{1, \frac{k_R}{k_{\min}}\big(1+\frac{|1-\theta|}{2k_R D}\big)\big\}}{\theta}\,\frac{k_{\max}^2}{k_{\min}^2}.$$

Proof. Let $u \in \mathcal{H}$ be given. We shall show that there exists $v_u \in \mathcal{H}$ such that

$$\operatorname{Re}\mathcal{B}(u, v_u) \gtrsim \|u\|_{\mathcal{H}}\|v_u\|_{\mathcal{H}},$$

where we use the notation $A \gtrsim B$ as a shorthand for the inequality $A \geq c\,B$, for some constant c. To this end, it is enough to show that: (a) $\operatorname{Re}\mathcal{B}(u, v_u) \gtrsim \|u\|^2_{\mathcal{H}}$, and (b) $\|u\|_{\mathcal{H}} \gtrsim \|v_u\|_{\mathcal{H}}$.

Let $v_u := \frac{1}{k^2_{\min}}u + z$, for some $z \in \mathcal{H}$. Then,

$$\begin{aligned}\mathcal{B}(u, v_u) &= \mathcal{B}\big(u, \frac{1}{k^2_{\min}}u + z\big) = \frac{1}{k^2_{\min}}\mathcal{B}(u, u) + \mathcal{B}(u, z)\\ &= \underbrace{\frac{1}{k^2_{\min}}\mathcal{B}(u, u) + 2\frac{k^2_{\max}}{k^2_{\min}}\|u\|^2}_{:=\mathrm{I}} + \underbrace{\mathcal{B}(u, z) - 2\frac{k^2_{\max}}{k^2_{\min}}\|u\|^2}_{:=\mathrm{II}}.\end{aligned}$$

Now we choose z such that the term II vanishes, i.e., let z be the solution of

$$\mathcal{B}(\phi, z) = 2\frac{k^2_{\max}}{k^2_{\min}}(\phi, u), \quad \text{for all } \phi \in \mathcal{H}. \tag{4.13}$$

Note that, since $\mathcal{H} \subset L^2(\Omega)$, the strong formulation associated to (4.13) reads: Find $z \in \mathcal{H}$ that satisfies the following adjoint boundary value problem with datum $2\frac{k^2_{\max}}{k^2_{\min}}u$,

$$\begin{aligned}-z'' - k^2(x)z &= 2\frac{k^2_{\max}}{k^2_{\min}}u, \quad x \in \Omega,\\ z'(x_L) &= ik_L z(x_L),\\ z'(x_R) &= -ik_R z(x_R).\end{aligned}$$

For (4.13), we may prove that the results of Proposition 4.2 still hold, thus z may be identified as the unique solution of (4.13) that satisfies the estimate (4.10). Hence,

$$\|z\|_{\mathcal{H}} \leq C_7\,\|u\|, \quad \text{where } C_7 := \frac{4\sqrt{2}D\max\left\{1, \frac{k_R}{k_{\min}}\left(1 + \frac{|1-\theta|}{2k_R D}\right)\right\}}{\theta}\,\frac{k^2_{\max}}{k^2_{\min}}.$$

Moreover, (3.4) implies that

$$\|z\|_{\mathcal{H}} \leq \frac{C_7}{k_{\min}}\,\|u\|_{\mathcal{H}}. \tag{4.14}$$

With this choice of z we have that

$$\operatorname{Re}\mathcal{B}(u, v_u) = \frac{1}{k^2_{\min}}\mathcal{B}(u, u) + 2\frac{k^2_{\max}}{k^2_{\min}}\|u\|^2 \overset{(3.7)}{\geq} \frac{1}{k^2_{\min}}\|u\|^2_{\mathcal{H}} - 2\frac{k^2_{\max}}{k^2_{\min}}\|u\|^2 + 2\frac{k^2_{\max}}{k^2_{\min}}\|u\|^2 = \frac{1}{k^2_{\min}}\|u\|^2_{\mathcal{H}}.$$

This shows that (a) holds. Specifically,

$$\operatorname{Re}\mathcal{B}(u, v_u) \geq \frac{1}{k^2_{\min}}\|u\|^2_{\mathcal{H}}. \tag{4.15}$$

Now,

$$\|v_u\|_{\mathcal{H}} = \left\|\frac{1}{k^2_{\min}}u + z\right\|_{\mathcal{H}} \leq \frac{1}{k^2_{\min}}\|u\|_{\mathcal{H}} + \|z\|_{\mathcal{H}} \overset{(4.14)}{\leq} \frac{1}{k^2_{\min}}\|u\|_{\mathcal{H}} + \frac{C_7}{k_{\min}}\,\|u\|_{\mathcal{H}} = \frac{1}{k_{\min}}\Big(\frac{1}{k_{\min}} + C_7\Big)\,\|u\|_{\mathcal{H}}.$$

Hence

$$\|u\|_{\mathcal{H}} \geq k_{\min}\Big(\frac{1}{k_{\min}} + C_7\Big)^{-1}\,\|v_u\|_{\mathcal{H}}, \tag{4.16}$$

and (4.15), (4.16), imply that

$$\operatorname{Re}\mathcal{B}(u, v_u) \geq \frac{1}{k^2_{\min}}\|u\|^2_{\mathcal{H}} \geq \frac{1}{k^2_{\min}}\|u\|_{\mathcal{H}}k_{\min}\Big(\frac{1}{k_{\min}} + C_7\Big)^{-1}\|v_u\|_{\mathcal{H}} = \frac{1}{k_{\min}}\Big(\frac{1}{k_{\min}} + C_7\Big)^{-1}\|u\|_{\mathcal{H}}\|v_u\|_{\mathcal{H}}.$$

□

5 Finite element approximation

In this section, as a proof of concept, we demonstrate that classical error estimates and quasi-optimality bounds can be derived for finite element approximations of our model problem. Since one of the aims of our approach is to significantly reduce the size of the computational domain, see the numerical results in Section 6, thereby enabling efficient methods for higher wavenumbers, we wanted to theoretically support the claim that the behaviour of the finite element method remains stable as expected. The material presented here can be derived using well-established arguments.

First, we derive error bounds for linear elements following Schatz [34], aiming to explicitly calculate the dependence of the mesh size restriction on k, see (5.7). Next, we extend our analysis to arbitrary discrete spaces, including any type of conforming finite elements, demonstrating quasi-optimal bounds and the discrete analog of the inf-sup stability condition (4.12). This analysis is based on ideas introduced in Aziz et al. [2], Makridakis et al. [24], Melenk [25], and adapts the approach from Schatz [34]. It also incorporates the notion of approximability of the dual problem introduced by Sauter [32], all of which are now considered standard arguments.

In Section 5.1, we explicitly work out the dependence on variable k in the involved constants. In Section 5.2, we provide a more general stability and quasi-optimality analysis. For a discussion on the restrictions and a comparison to existing results, see Remarks 5.1, 5.2.

5.1 Convergence for linear elements

In what follows we use the classical ideas of Schatz [34]. For $0 < h < 1$, let S_h be a finite-dimensional subspace of continuous, piecewise polynomial functions in H^1. We assume that for every $v \in H^2(\Omega)$ the following approximation property holds

$$\inf_{\phi \in S_h} \{\|v - \phi\| + h\|v' - \phi'\|\} \le C_8\, h^2 \|v''\|. \tag{5.1}$$

In the sequel, C will denote generic constants, not necessarily the same at any two different places, that are independent of k. Let u_h be the solution of

$$\mathcal{B}(u_h, \phi) = e^{ik_L d}\overline{\phi}(x_L), \quad \forall \phi \in S_h. \tag{5.2}$$

Let us denote $e_h := u - u_h$. Then, Gårding's inequality (3.7) implies that

$$\operatorname{Re}\mathcal{B}(e_h, e_h) \ge \|e_h\|_{\mathcal{H}}{}^2 - 2\,k_{\max}^2\|e_h\|^2 \;\Leftrightarrow\; \|e_h\|_{\mathcal{H}}{}^2 \le \operatorname{Re}\mathcal{B}(e_h, e_h) + 2\,k_{\max}^2\|e_h\|^2.$$

Note that $\mathcal{B}(e_h, \phi) = 0$, for all $\phi \in S_h$. Hence for C_4 defined as in (3.6)

$$\begin{aligned}
|\mathcal{B}(e_h, e_h)| &= |\mathcal{B}(e_h, u - \phi)| \\
&\le \|e_h'\|\|(u-\phi)'\| + \|ke_h\|\|u - \phi\| + k_R\,|e_h(x_R)||(u-\phi)(x_R)| + k_L\,|e_h(x_L)||(u-\phi)(x_L)| \\
&\le \|e_h'\|\|(u-\phi)'\| + \|ke_h\|\|u - \phi\| + k_R\,|e_h(x_R)||(u-\phi)(x_R)| + k_L\,|e_h(x_L)||(u-\phi)(x_L)| \\
&\overset{(5.1),(3.5)}{\le} C_8 h\,\|e_h'\|\|u''\| + C_8 h^2\|ke_h\|\|u''\| + k_R\,\frac{C_3}{\sqrt{k_{\min}}}\|e_h\|_{\mathcal{H}} C_2 \|u-\phi\|^{1/2}\|u-\phi\|_1^{1/2} \\
&\quad + k_L\,\frac{C_3}{\sqrt{k_{\min}}}\|e_h\|_{\mathcal{H}} C_2 \|u-\phi\|^{1/2}\|u-\phi\|_1^{1/2} \\
&= 2\sqrt{\varepsilon}\,\|e_h'\|\,\frac{C_8 h}{2\sqrt{\varepsilon}}\,\|u''\| + 2\sqrt{\varepsilon}\,\|ke_h\|\,\frac{C_8 h^2}{2\sqrt{\varepsilon}}\,\|u''\| + 2\sqrt{\varepsilon}\,\|e_h\|_{\mathcal{H}}\, C_2 C_3 C_8^2\,\frac{k_L + k_R}{2\sqrt{\varepsilon}\sqrt{k_{\min}}}\,h^{3/2}\|u''\|^2 \\
&\le \varepsilon\,\|e_h'\|^2 + C_8^2\frac{h^2}{4\varepsilon}\|u''\|^2 + \varepsilon\,\|ke_h\|^2 + C_8^2\frac{h^4}{4\varepsilon}\|u''\|^2 + \varepsilon\,\|e_h\|_{\mathcal{H}}^2 \\
&\quad + C_2^2 C_3^2 C_8^4\,\frac{(k_L + k_R)^2}{4\varepsilon k_{\min}}\,h^3\|u''\|^2 \\
&\le 2\varepsilon\|e_h\|_{\mathcal{H}}^2 + C\Big(\frac{h^2}{4\varepsilon} + \frac{h^4}{4\varepsilon} + C_3^2\,\frac{(k_L + k_R)^2}{k_{\min}}\,\frac{h^3}{4\varepsilon}\Big)\|u''\|^2.
\end{aligned}$$

Hence

$$\begin{aligned}
\|e_h\|_{\mathcal{H}}{}^2 &\le\; \operatorname{Re}\mathcal{B}(e_h, e_h) + 2\,k_{\max}\|e_h\|^2 \le |\mathcal{B}(e_h, e_h)| + 2\,k_{\max}^2\|e_h\|^2 \\
&\le 2\varepsilon\|e_h\|_{\mathcal{H}}{}^2 + C\Big(\frac{h^2}{4\varepsilon} + C_3^2\,\frac{(k_L + k_R)^2}{k_{\min}}\,\frac{h^3}{4\varepsilon} + \frac{h^4}{4\varepsilon}\Big)\|u''\|^2 + 2\,k_{\max}^2\|e_h\|^2.
\end{aligned}$$

Choosing $\varepsilon = 1/4$ shows that

$$\frac{1}{2}\|e_h\|_{\mathcal{H}}{}^2 \le C\Big(1 + C_3^2\,\frac{(k_L+k_R)^2}{k_{\min}}\,h + h^2\Big)\,h^2\,\|u''\|^2 + 2\,k_{\max}^2\|e_h\|^2. \tag{5.3}$$

Now let $z \in \mathcal{H}$ be the solution of the adjoint problem

$$\mathcal{B}(\psi, z) = k_{\max}^2(\psi, e_h), \quad \text{for all } \psi \in \mathcal{H}. \tag{5.4}$$

Then, (4.11) shows that

$$\|z''\| \le (1 + C_6 k_{\max})k_{\max}^2\|e_h\|. \tag{5.5}$$

Let $\chi \in S_h$. Equation (5.4) for $\psi = e_h$ implies that

$$k_{\max}^2\|e_h\|^2 = \mathcal{B}(e_h, z) = \mathcal{B}(e_h, z-\chi) \overset{(3.6)}{\le} C_4\|e_h\|_{\mathcal{H}}\|z-\chi\|_{\mathcal{H}}.$$

Notice that

$$\begin{aligned}\|z-\chi\|_{\mathcal{H}}{}^2 &= \|(z-\chi)'\|^2 + \|k(z-\chi)\|^2 \le \|(z-\chi)'\|^2 + k_{\max}^2\|z-\chi\|^2\\ &\overset{(5.1)}{\le} C_8^2\,h^2\|z''\|^2 + C_8^2\,k_{\max}^2 h^4\|z''\|^2 = C\,\big(1 + h^2k_{\max}^2\big)h^2\|z''\|^2.\end{aligned}$$

Therefore

$$k_{\max}^2\|e_h\|^2 \le CC_4\|e_h\|_{\mathcal{H}}\big(1+h^2k_{\max}^2\big)^{1/2}h\|z''\| \overset{(5.5)}{\le} CC_4\|e_h\|_{\mathcal{H}}\big(1+h^2k_{\max}^2\big)^{1/2}h\,(1+C_6k_{\max})\,k_{\max}^2\|e_h\|,$$

from which we conclude that

$$\|e_h\| \le CC_4\big(1+h^2k_{\max}^2\big)^{1/2}(1+C_6k_{\max})\,h\,\|e_h\|_{\mathcal{H}}. \tag{5.6}$$

Hence, by (5.3) and (5.6) we obtain

$$\begin{aligned}\frac{1}{2}\|e_h\|_{\mathcal{H}}{}^2 &\le C\Big(1 + C_3^2\,\frac{(k_L+k_R)^2}{k_{\min}}\,h + h^2\Big)\,h^2\,\|u''\|^2 + 2\,k_{\max}^2\|e_h\|^2\\ &\le C\Big(1 + C_3^2\,\frac{(k_L+k_R)^2}{k_{\min}}\,h + h^2\Big)\,h^2\,\|u''\|^2 + 2C^2C_4^2\big(1+h^2k_{\max}^2\big)(1+C_6k_{\max})^2k_{\max}^2h^2\|e_h\|_{\mathcal{H}}{}^2.\end{aligned}$$

Equivalently,

$$\underbrace{\Big(\frac{1}{2} - 2C^2C_4^2\big(1+h^2k_{\max}^2\big)(1+C_6k_{\max})^2k_{\max}^2h^2\Big)}_{=\mathcal{C}}\,\|e_h\|_{\mathcal{H}}{}^2 \le C\Big(1 + C_3^2\,\frac{(k_L+k_R)^2}{k_{\min}}\,h + h^2\Big)\,h^2\,\|u''\|^2.$$

Then, provided that h is small enough so that

$$\Big(\frac{1}{2} - 2C^2C_4^2\big(1+h^2k_{\max}^2\big)(1+C_6k_{\max})^2k_{\max}^2h^2\Big) = \mathcal{C} \ge \frac{1}{4}\,, \tag{5.7}$$

the following H^1–estimate holds

$$\|e_h\|_{\mathcal{H}} \le C(k,h)\,h\,\|u''\|.$$

The corresponding L^2–estimate follows from (5.6):

$$\|e_h\| \le C(k,h)\,h^2\,\|u''\|.$$

5.2 Convergence for general discrete spaces

The results below are based on general discrete spaces V_h, which are finite-dimensional subspaces capable of approximating efficiently solutions to our model. Without loss of generality, we denote by h the generic discretisation parameter, not necessarily associated with the mesh size. It will be instrumental to use the dual problem: for $g \in L^2$ let $z \in \mathcal{H}$ be the solution of the adjoint problem

$$\mathcal{B}(\psi, z) = (\psi, g), \quad \text{for all } \psi \in \mathcal{H}. \tag{5.8}$$

Let T be the solution operator $T : L^2 \to \mathcal{H}$, i.e., $z = Tg$. The main idea in Sauter [32] is to introduce the quantity

$$\eta(V_h) = \sup_{0\neq g\in L^2} \inf_{\chi\in V_h} \frac{\|T\,g-\chi\|_{\mathcal{H}}}{\|g\|}. \tag{5.9}$$

We shall assume that $\eta(V_h) \to 0$ as $h \to 0$. Denoting $\varPsi = T(u - u_h)$, where $u_h \in V_h$ is the solution of the discrete problem

$$\mathcal{B}(u_h, \phi) = e^{ik_L d}\overline{\phi}(x_L), \quad \forall \phi \in V_h, \tag{5.10}$$

we have that

$$\|e_h\|^2 = \mathcal{B}(e_h, \varPsi) = \mathcal{B}(e_h, \varPsi - \chi) \le C_4 \|e_h\|_{\mathcal{H}} \|\varPsi - \chi\|_{\mathcal{H}}.$$

Therefore,

$$\|e_h\| \le C_4\, \eta(V_h)\, \|e_h\|_{\mathcal{H}}.$$

Hence, for any $\phi \in V_h$,

$$\begin{aligned}\|e_h\|_{\mathcal{H}}{}^2 \le\ & \operatorname{Re}\mathcal{B}(e_h, e_h) + 2\,k_{\max}^2 \|e_h\|^2 \le |\mathcal{B}(e_h, e_h)| + 2\,k_{\max}^2\|e_h\|^2\\ &\le |\mathcal{B}(e_h, u-\phi)| + 2\,(C_4\,\eta(V_h)\,)^2 k_{\max}^2\, \|e_h\|_{\mathcal{H}}{}^2.\end{aligned}$$

Therefore we conclude that

$$\|u - u_h\|_{\mathcal{H}} \le 2C_4 \inf_{\chi\in V_h} \|u - \chi\|_{\mathcal{H}}, \tag{5.11}$$

provided the discrete spaces are chosen for sufficiently small h so that the following condition is satisfied:

$$(C_4\,\eta(V_h)\,)^2 k_{\max}^2 \le \frac{1}{4}\,. \tag{5.12}$$

This condition, for constant wavenumber k, is the same as that used in the work of Sauter [32]. Under similar restrictions on η, one may prove the discrete analog of the inf-sup condition, i.e., for all $\psi \in V_h$, there holds

$$\sup_{0\neq v\in V_h} \frac{\operatorname{Re}\mathcal{B}(\psi, v)}{\|v\|_{\mathcal{H}}} \ge \frac{\alpha}{k_{\min}} \Big(\frac{1}{k_{\min}} + C_7\Big)^{-1} \|\psi\|_{\mathcal{H}}, \tag{5.13}$$

where α is independent of k and the constant C_7 is defined in (4.12). Notably, (5.13) implies quasi-optimal bounds but with constants that depend on the inverse of the inf-sup constant in (5.13). For interesting discussions on this issue, see [18, 24]. Analogous differences on the stability and quasi-optimality constants appear in [32, 26].

Remark 5.1. The main ideas of the proofs of inf-sup stability and quasi-otimality using variational arguments can be traced back to Aziz et al. [2] (quasioptimality), Makridakis et al. [24] (discrete inf-sup), and with a slightly different proof in Melenk [25]. Discrete stability using discrete Green's function was established by Ihlenburg and Babuska [18] . The variational arguments were enriched by the interesting idea of Sauter [32] to include the approximability of the dual problem in an abstract form, described above. This was important, since it allowed a series of developments regarding the concrete assessment of restrictions of the type (5.12) for each discrete space. For example, in the case of Helmholtz equation with constant coefficients and constant k, [26] demonstrated that the h-p finite element method yields quasi-optimality and discrete stability provided hk is sufficiently small and $p \ge C \log k$. These results are based on explicit representations of the solution of the dual problem with right-hand side in the discrete space and do not extend straightforwardly to other cases of interest, such as when variable coefficients and wavenumbers are considered. Recent developments in this direction include, e.g., [6, 11].

Remark 5.2. The quasi-optimality bound (5.11) is very similar to the one derived in Theorem 4.2 of Graham and Sauter [15], although the definition of $\eta(V_h)$ is slightly different. In Theorem 4.5 of [15], concrete bounds for $\eta(V_h)$ are derived for finite element spaces that satisfy the analog of (5.1). It is interesting to note, as expected, the similarity of the corresponding mesh restrictions to those required to establish the bound in Section 5.1, as a consequence of the analog of (5.12). These restrictions, roughly speaking, require k^2h to be sufficiently small which is known to be an irreducible constraint for linear elements.

6 Numerical experiments

In this section we comment on the outcome of some numerical experiments performed with a code that implements a finite element method with piecewise linear, quadratic or cubic basis functions, for the solution of (3.3) with a variable wavenumber. In the case of a constant wavenumber k_0, a direct comparison of the numerical solution with the exact solution of the problem $u(x) = i/(2k_0)\exp(ik_0|x - x_s|)$, confirmed the expected rates of convergence in the L^2 and $\|\cdot\|_{\mathcal{H}}$ norms.

Here, we consider a variable wavenumber $k(x) = 2\pi f_s/c(x)$, where f_s is the frequency of the harmonic source (in Hz) and $c(x)$ is the sound speed (in m/s). In all test cases reported below, the frequency is set to $f_s = 4.2$ kHz, the source is located at $x_s = -10$, and the sound speed varies within the interval $[x_1, x_2] = [5, 15]$, where all distances are in meters. The results shown below were obtained for a uniform discretization of the interval $[x_L, x_R]$ with N elements and piecewise linear basis functions.

Test case 1. In our first experiment we consider a sound speed that is equal to $c_1 = 5500$ m/s for $x < x_1$, decreases linearly from c_1 to $c_2 = 2500$ m/s in $[x_1, x_2]$, and is equal to c_2 for $x > x_2$. This corresponds to a wavenumber k that increases from $k_L(x_1) \approx 4.80$ to $k_R(x_2) \approx 10.56$, see the graph in the left subplot of Figure 3. The right plot of Figure 3 shows the modulus of the approximate solution u_h in a logarithmic scale for the vertical axis. The two line colours, blue and red, correspond to the numerical solution computed on a uniform partition of $[x_L, x_R] = [-5, 25]$ with $N = 15000$ elements and a uniform partition of $[x_L, x_R] = [0, 20]$ with $N = 10000$ elements, respectively. In Figure 4 we plot the

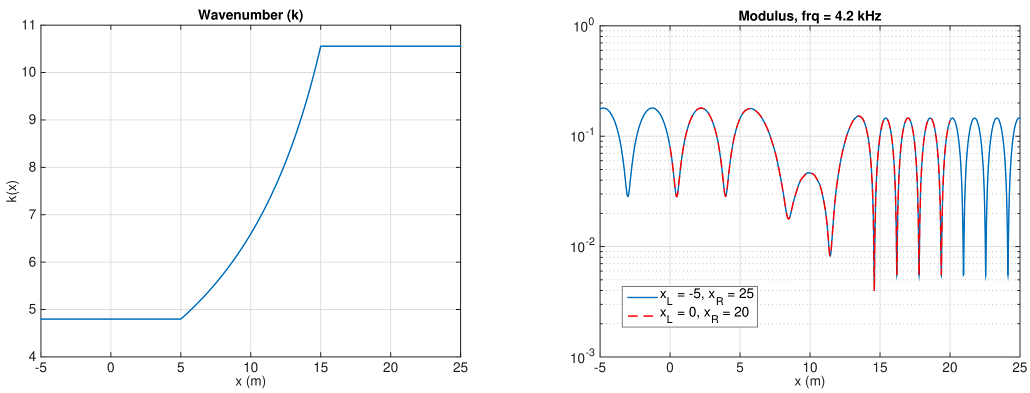

Figure 3: The graph of the wavenumber (left) and the modulus of u_h (right) for a linearly decreasing sound speed profile and two different locations of the artificial boundaries.

real (left subplot) and the imaginary part (right subplot) of the finite element solution u_h for the same two locations of the artificial boundaries. A direct numerical comparison indicates that the quality of the approximation is independent of the location of the artificial boundaries.

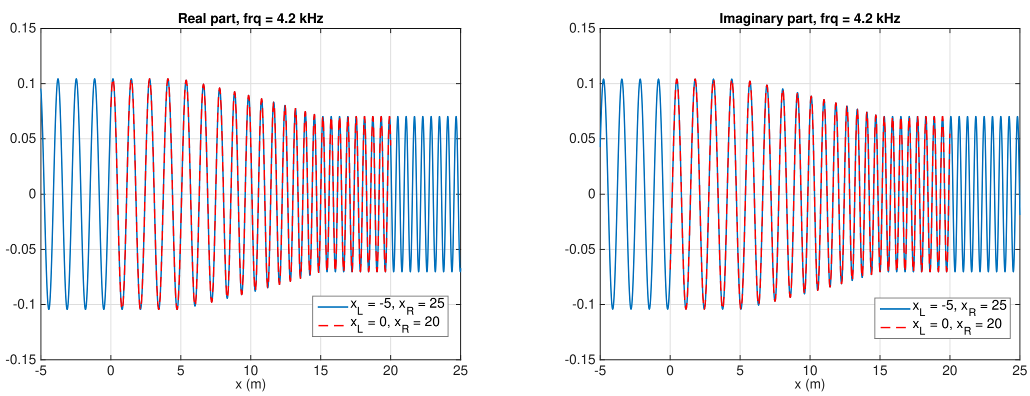

Figure 4: Real part (left) and imaginary part (right) of the numerical solution for a linearly decreasing sound speed profile and two different locations of the artificial boundaries.

Test case 2. Here we consider a sound speed that increases linearly from $c_1 = 2500$ m/s to $c_2 = 5500$ m/s in $[x_1, x_2]$, while it is equal to c_1 for $x < x_1$, and to c_2 for $x > x_2$, respectively. The wavenumber k decreases from $k_L(x_1) \approx 10.56$ to $k_R(x_2) \approx 4.80$ and is depicted in the left subplot of Figure 5. In the right plot of Figure 5 we present the modulus of the approximate solution u_h in a logarithmic scale for the vertical axis, for the same locations of the artificial boundaries as in the previous test case. The two line colours, blue and red, correspond to the numerical solution computed on a uniform partition of $[x_L, x_R] = [-5, 25]$ with $N = 15000$ elements and a uniform partition of $[x_L, x_R] = [0, 20]$ with $N = 10000$ elements, respectively. The corresponding real and imaginary parts are shown in the left and right subplots of Figure 6, respectively. Numerical comparisons verifies the excellent agreement between the two solution curves and confirms the efficiency of the proposed approach.

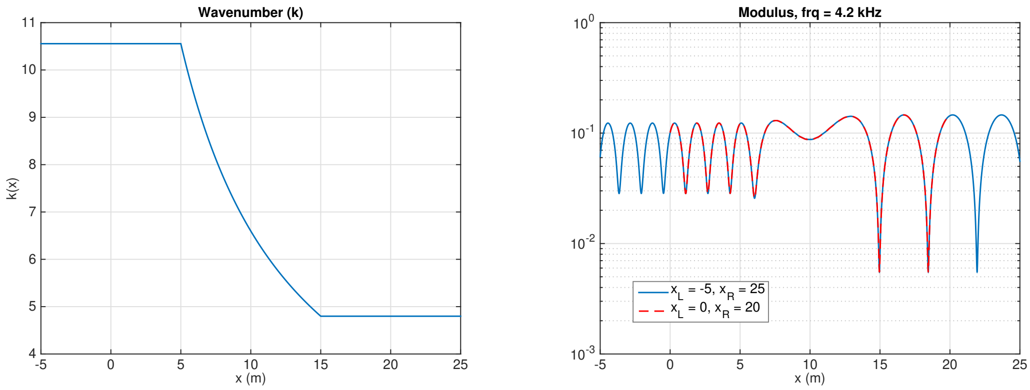

Figure 5: The graph of the wavenumber (left) and the modulus of u_h (right) for a linearly increasing sound speed profile and two different locations of the artificial boundaries.

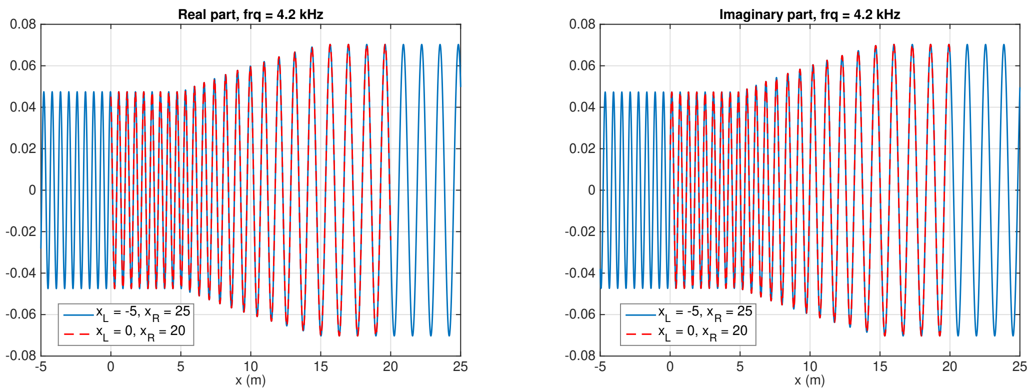

Figure 6: Real part (left) and imaginary part (right) of the numerical solution for a linearly increasing sound speed profile and two different locations of the artificial boundaries.

Test case 3. As a more challenging numerical experiment we consider an oscillatory sound speed profile defined by

$$c(x) = \begin{cases} 5500 & \text{for } x < x_1, \\ 5500 - 3000\big[x - x_1 + \sin\big(5\pi(x - x_1)\big)\big]/(x_2 - x_1) & \text{for } x_1 \le x \le x_2, \\ 2500 & \text{for } x > x_2. \end{cases} \tag{6.1}$$

The graph of the wavenumber k for the sound speed defined in (6.1) appears in the left plot in Figure 7. The right plot of Figure 7 shows the modulus of the approximate solution u_h in a logarithmic scale for the vertical axis. The two line colours, blue and red, correspond to the numerical solution computed on a uniform partition of $[x_L, x_R] = [-5, 25]$ with $N = 15000$ elements and a uniform partition of $[x_L, x_R] = [0, 20]$ with $N = 10000$ elements, respectively. In Figure 8 we plot the real and imaginary parts of u_h computed with the same two different locations of the artificial boundaries.

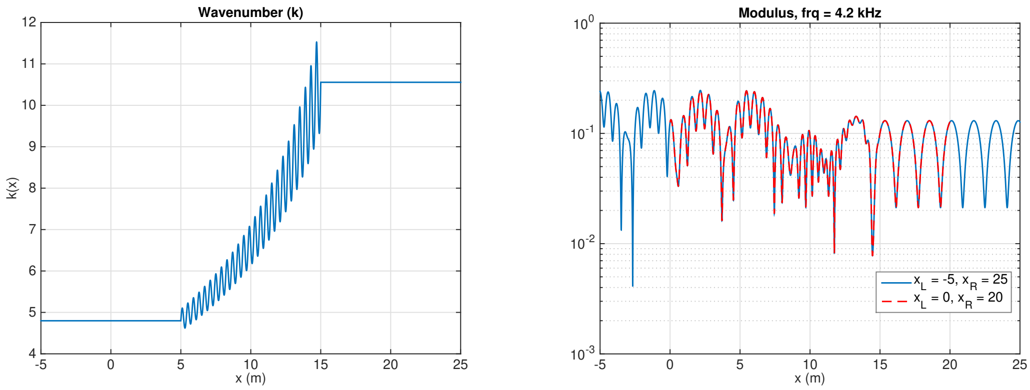

Figure 7: The graph of the wavenumber (left) and the modulus of u_h (right) for the sound speed profile (6.1) and two different locations of the artificial boundaries.

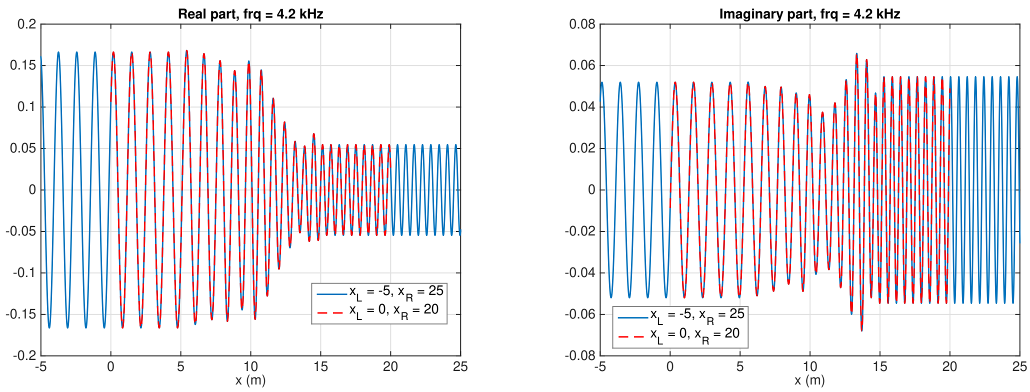

Figure 8: Real part (left) and imaginary part (right) of the numerical solution for the sound speed profile (6.1) for different locations of the artificial boundaries.

Test case 4. As a final example, we consider a sound speed defined by

$$c(x) = \begin{cases} 2500 & \text{for } x < x_1, \\ 2500 + 3000\big[x - x_1 + \sin\big(5\pi(x - x_1)\big)\big]/(x_2 - x_1) & \text{for } x_1 \leq x \leq x_2, \\ 5500 & \text{for } x > x_2. \end{cases} \tag{6.2}$$

The graph of the wavenumber k for the sound speed defined in (6.2) appears in the left plot in Figure 9. The right plot of Figure 9 shows the modulus of the approximate solution u_h in a logarithmic scale for the vertical axis. The two line colours, blue and red, correspond to the numerical solution computed on a uniform partition of $[x_L, x_R] = [-5, 25]$ with $N = 15000$ elements and a uniform partition of $[x_L, x_R] = [0, 20]$ with $N = 10000$ elements, respectively. In Figure 10 we plot the real and imaginary parts of u_h computed with the same two different locations of the artificial boundaries.

From the test cases presented here, and from the outcome of many other experiments with different sound speed profiles and with finite element spaces with piecewise quadratic or cubic basis functions, we can conclude that the truncation of the domain and the introduction of an artificial boundary near the source leads to an efficient method which requires only a small number of elements, and captures the wave propagation well. It is worth mentioning that although in the last three test cases the virial condition (4.1) *does not hold*, the computation of the numerical solution is still effective, and the quality of the approximation is excellent, independently of the location of the artificial boundaries.

A final note concerns the modulus of the computed solution shown in Figures 3, 5, 7, and 9. As expected, outside the interval $(x_1, x_2) = (5, 15)$ where k is constant it appears to be periodic while within the interval is aperiodic due to the scattering of the wave by the inhomogeneity. It turns out that the scattering effect is stronger and the oscillations of the solution are profound in the presence of rough

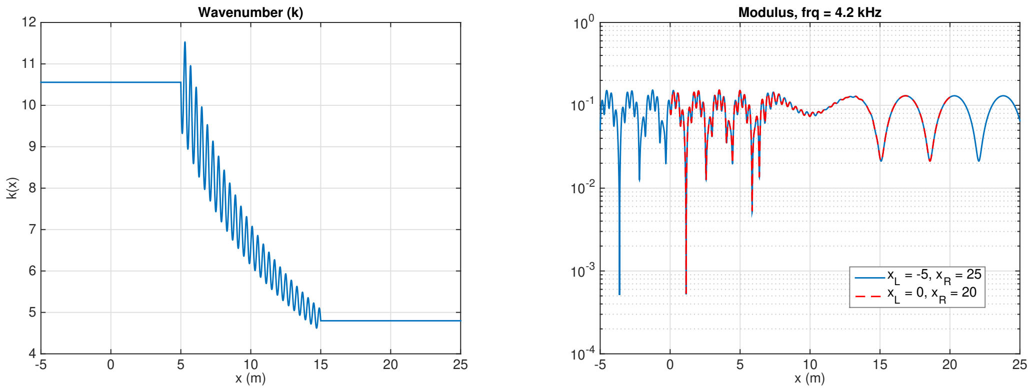

Figure 9: The graph of the wavenumber (left) and the modulus of u_h (right) for the sound speed profile (6.2) for different locations of the artificial boundaries.

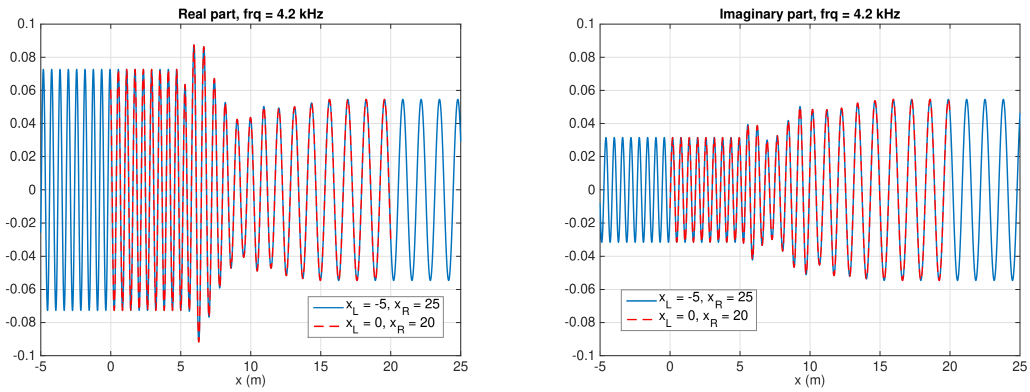

Figure 10: Real part (left) and imaginary part (right) of the numerical solution for the sound speed profile (6.2) for different locations of the artificial boundaries.

oscillations in the wave speed, the worst case among the test cases that we have presented here appears for a rough inhomogeneity where the wavenumber decreases in an oscillatory way (Figure 9).

References

[1] G. A. Athanassoulis, K.A. Belibassakis, D. A. Mitsoudis, N.A. Kampanis, and V. A. Dougalis. Coupled mode and finite element approximations of underwater sound propagation problems in general stratified environments. *Journal of Computational Acoustics*, 16(1):83–116, 2008.

[2] A. K. Aziz, R. B. Kellogg, and A. B. Stephens. A two point boundary value problem with a rapidly oscillating solution. *Numerische Mathematik*, 53(1-2):107–121, 1988.

[3] A. Bayliss, C.I Goldstein, and E. Turkel. On accuracy conditions for the numerical computation of waves. *Journal of Computational Physics*, 59(3):396–404, 1985.

[4] Eliane Bécache and Maryna Kachanovska. Stability and convergence analysis of time-domain perfectly matched layers for the wave equation in waveguides. *SIAM Journal on Numerical Analysis*, 59(4):10.1137/20M1330543, 2021.

[5] Abderrahmane Bendali and Phillippe Guillaume. Non-reflecting boundary conditions for waveguides. *Mathematics of Computation*, 68(225):123–144, 1999.

[6] T Chaumont-Frelet and S Nicaise. Wavenumber explicit convergence analysis for finite element discretizations of general wave propagation problems. *IMA Journal of Numerical Analysis*, 40(2):1503–1543, 05 2019.

[7] Théofile Chaumont-Frelet. On high order methods for the heterogeneous helmholtz equation. *Computers and Mathematics with Applications*, 72(9):2203–2225, 2016.

[8] Peter Cummings and Xiaobing Feng. Sharp regularity coefficient estimates for complex-valued acoustic and elastic helmholtz equations. *Mathematical Models and Methods in Applied Sciences*, 16(01):139–160, 2006.

[9] S. Dyatlov and M. Zworski. *Mathematical Theory of Scattering Resonances*, volume 200 of *Graduate Studies in Mathematics*. American Mathematical Society Providence, Rhode Island, 2019.

[10] George J. Fix and Samuel P. Marin. Variational methods for underwater acoustic problems. *Journal of Computational Physics*, 28(2):253–270, 1978.

[11] Jeffrey Galkowski and Euan A. Spence. Sharp preasymptotic error bounds for the helmholtz h-fem. arXiv2301.03574, 2023.

[12] Dan Givoli. *Numerical methods for problems in infinite domains*. Elsevier, New York, 1992.

[13] Charles I. Goldstein. A finite element method for solving helmholtz type equations in waveguides and other unbounded domains. *Mathematics of Computation*, 39(160):309–324, 1982.

[14] I.G. Graham, O.R. Pembery, and E.A. Spence. The helmholtz equation in heterogeneous media: A priori bounds, well-posedness, and resonances. *Journal of Differential Equations*, 266(6):2869–2923, 2019.

[15] I.G. Graham and S.A. Sauter. Stability and finite element error analysis for the helmholtz equation with variable coefficients. *Mathematics of Computation*, 89(321):105–138, 2020.

[16] P.D. Hislop and I.M. Sigal. *Introduction to Spectral Theory: With Application to Schrödinger Operators*, volume 113 of *Applied Mathematical Sciences*. Springer-Verlag, 1996.

[17] Frank Ihlenburg. *Finite Element Analysis of Acoustic Scattering*, volume 132 of *Applied Mathematical Sciences*. Springer New York, NY, 1998.

[18] Frank Ihlenburg and Ivo M. Babuška. Finite element solution of the helmholtz equation with high wave number part i: The h-version of the fem. *Computers & Mathematics with Applications*, 30(9):9–37, 1995.

[19] Finn B. Jensen, William A. Kuperman, Michael B. Porter, and Henrik Schmidt. *Computational Ocean Acoustics*. Springer New York, NY, 2nd edition, 2011.

[20] Joseph B. Keller and Dan Givoli. Exact non-reflecting boundary conditions. *Journal of Computational Physics*, 82(1):172–192, 1989.

[21] Seungil Kim. Error analysis of pml-fem approximations for the helmholtz equation in waveguides. *ESAIM: M2AN*, 53(4):1191–1222, 2019.

[22] V.V. Kucherenko. The short-wave asymptotic behavior of green's function for the n-dimensional wave equation in an inhomogeneous medium. *USSR Comp. Math. Math. Phys.*, 8(4):294–302, 1968.

[23] V.V. Kucherenko. Quasiclassical asymptotics of a point-source function for the stationary schrödinger equation. *Theor. Math. Phys.*, 1(3):294–310, 1969.

[24] Charalambos Makridakis, Frank Ihlenburg, and Ivo Babuška. Analysis and finite element methods for a fluid-solid interaction problem in one dimension. *Mathematical Models and Methods in Applied Sciences*, 6(8):1119–1141, 1996.

[25] Jens Markus Melenk. *On Generalized Finite Element Methods*. PhD thesis, University of Maryland, University of Maryland, College Park, MD, 1995.

[26] J.M. Melenk and S.A. Sauter. Convergence analysis for finite element discretizations of the helmholtz equation with dirichlet-to-neumann boundary conditions. *Mathematics of Computation*, 79(272):1871–1914, 2010.

[27] Dimitrios A. Mitsoudis. Near- and far-field boundary conditions for a finite element method for the helmholtz equation in axisymmetric problems of underwater acoustics. *Acta Acustica united with Acustica*, 93(6):888–898, 2007.

[28] Dimitrios A. Mitsoudis, Charalambos Makridakis, and Michael Plexousakis. Helmholtz equation with artificial boundary conditions in a two-dimensional waveguide. *SIAM Journal on Mathematical Analysis*, 44(6):4320–4344, 2012.

[29] Dimitrios A. Mitsoudis and M. Plexousakis. A finite element method with nonlocal boundary conditions for the helmholtz equation with complex wavenumber in stratified waveguides. *Acta Acustica united with Acustica*, 95(4):753–756, 2009.

[30] C. S. Morawetz and D. Ludwig. An inequality for the reduced wave operator and the justification of geometrical optics. *Communications on Pure and Applied Mathematics*, 21(2):187–203, 1968.

[31] A. G. Ramm. *Scattering by Obstacles and Potentials*. World Scientific Singapore, 2000.

[32] S. A. Sauter. A refined finite element convergence theory for highly indefinite helmholtz problems. *Computing*, 78(139):101–115, 2006.

[33] Stefan Sauter and Céline Torres. Stability estimate for the helmholtz equation with rapidly jumping coefficients. *Zeitschrift für angewandte Mathematik und Physik*, 69(139), 2018.

[34] Alfred H. Schatz. An observation concerning ritz-galerkin methods with indefinite bilinear forms. *Mathematics of Computation*, 28(128):959–962, 1974.

[35] I. Singer and E. Turkel. A perfectly matched layer for the helmholtz equation in a semi-infinite strip. *Journal of Computational Physics*, 201(2):439–465, 2004.

[36] D. R. Yafaev. *Scattering Theory: Some Old and New Problems*, volume 1735 of *Lecture Notes in Mathematics*. Springer-Verlag Berlin Heidelberg, 2000.